Radiation Physics and Chemistry 179 (2021) 109207

Contents lists available at ScienceDirect

Radiation Physics and Chemistry

journal homepage: www.elsevier.com/locate/radphyschem

Application of the Reduced-Fitting Method to determine neutron scattering

Tallyson S. Alvarenga[a,*], Ivon O. Polo[a], Walsan W. Pereira[b], Michael R. Mayhugh[c], Linda V.E. Caldas[a]

[a] Instituto de Pesquisas Energéticas e Nucleares/ Comissão Nacional de Energia Nuclear, IPEN/CNEN, Av. Prof. Lineu Prestes, 2242, 05508-000, São Paulo, SP, Brazil
[b] Instituto de Radioproteção e Dosimetria/ Comissão Nacional de Energia Nuclear, IRD/CNEN, Av. Salvador Allende, 9, 22780-160, Rio de Janeiro, RJ, Brazil
[c] Faceted Development, LLC, 3641 Rawnsdale Rd. Shaker Hts, OH, 44122, USA

ARTICLE INFO

Keywords:
Neutron scattering
Neutron calibration
Neutron spectrum

ABSTRACT

As the number of techniques using neutron radiation has grown, the number of neutrons detectors has increased along with need for their calibration. In Brazil this substantial demand for neutron detector calibration falls on a single laboratory located in Rio de Janeiro. One of the major problems in the calibration of neutron detectors is neutron scattering, which varies depending on the size and configuration of the laboratory. This is due to the neutrons that interact with the experimental setup and the surrounding, walls, floor and ceiling. This scatter influences the reading of the instrument to be calibrated and causes systematic errors in the calibration of neutron detectors. ISO 8529-2 recommends the following methods to correct these effects: The Semi-Empirical Method (SEM), the Reduced-Fitting Method (RFM), the Shadow-Cone Method (SCM) and the Generalized Fit Method (GFM). In this study, the neutron scattering characterization was performed in the Neutron Calibration Laboratory (LCN) of IPEN/CNEN, using the RFM method. The neutron source used was 241AmBe, which was positioned in the center of the calibration room. Neutron spectra were obtained using a scintillation detector based on 6Lil(Eu) in combination with a Bonner sphere spectrometer (BSS) at source-detector distances from 30 cm to 258 cm.

1. Introduction

The use of neutron radiation is increasing with a corresponding growth in the importance of the associated radiation protection including area monitoring and improving the safety of installations and operators. Reliable measurement of neutron radiation is a very difficult task due to the large energy range and complex interactions with matter (Schuhmacher, 2004; Le et al., 2017). The calibration of radiation detectors, such as survey meters and individual dosimeters, is performed with the aim of ensuring accurate measurements including determination of the associated uncertainties, taking into account the requirements established by the regulatory authorities.

In practical situations involving the calibration of neutron detectors, one of the main problems is neutron scattering, which varies with the size and configuration of the calibration laboratory (Kluge et al., 1997; Alvarenga et al., 2017). The neutron spectrum (and the reference ambient dose equivalent rates), measured at a certain point in the calibration laboratory is not the same spectrum as that emitted by and arriving directly from the neutron source, due to the addition of scattered neutrons which influence the reading of the instrument to be calibrated and cause systematic errors in the calibration of the neutron detectors (Schuhmacher, 2004; Lee et al., 2018).

To avoid these errors, the calibration laboratory would need to be free of neutron scattering; however, in practice, it is impossible to obtain such conditions since there are scattered neutrons from the interaction of radiation with the experimental set-up, walls, floor, ceiling, and air (Gressier, 2014; Dawn et al., 2016; Le et al., 2017). To choose a reliable method for evaluating neutron scattering, several factors must be analyzed, including: source type, detector geometry, calibration distance and laboratory dimensions (Lee et al., 2018; Hwan et al., 2014).

The determination of scattering radiation can occur through simulation using the Monte Carlo Code (MCNP), which allows a more detailed evaluation of the interaction of neutrons with air and structural components of the laboratory (Lee et al., 2018; Thiem et al., 2017; Vega-Carrillo et al., 2007a, 2007b), following the recommendations of ISO 8529-2 (ISO, 2000). Currently, there are four standard methods recommended by ISO 8529-2 (ISO, 2000) to determine neutron scattering. They are called the Semi-Empirical Method (SEM), the Reduced-Fitting Method (RFM), and the Generalized Fit Method (GFM), which

* Corresponding author.
E-mail address: tallysonalvarenga@gmail.com (T.S. Alvarenga).

https://doi.org/10.1016/j.radphyschem.2020.109207
Received 13 February 2020; Received in revised form 10 September 2020; Accepted 21 September 2020
Available online 23 September 2020
0969-806X/

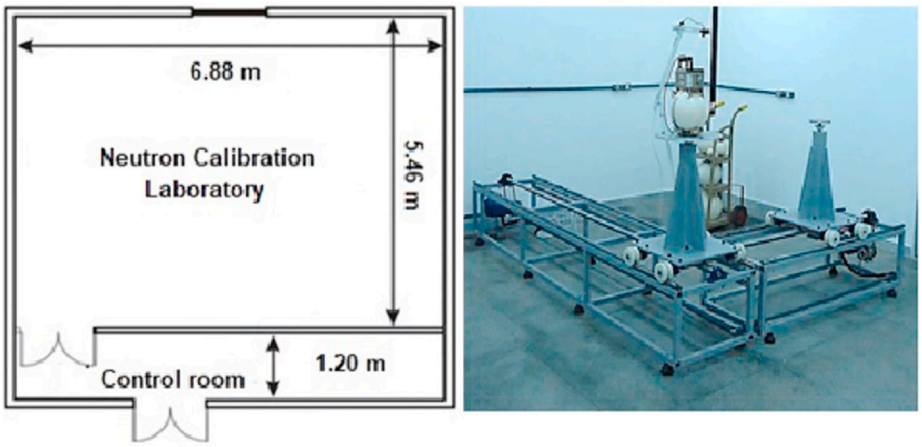

Fig. 1. Simplified floor plan of the Neutron Calibration Laboratory and the set-up used to vary the distance between the detector and the source.

are based on consecutive measurements varying the source-detector distance, and the Shadow Cone Method, which is based on the measurement at the location selected for measurement (ISO, 2000).

The RFM is a simplified method that may be used if the minimum value of distance is at least, approximately 1.5 times the largest dimension of the device to be calibrated. Under these conditions one can assume that the scattering in air correction term is negligible compared to the dispersion from the room.

Knowledge of the neutron scattering spectrum is desirable, but it is not essential for neutron device calibrations. The study of the neutron field can be performed using a Bonner sphere spectrometer (BSS), which has been widely used in neutron spectrometry (Antanackovic et al., 2015). This system consists of a thermal neutron detector, located in the center of the moderating spheres, with different diameters. These spheres are composed of high density polyethylene, which allow the recording of different neutron counts and different response curves as a function of energy. The thermal neutron detectors most used at the center of the moderating spheres are based on: 3He, BF3, 6Lil (Eu) and thermoluminescent detectors (TL), which have been shown to be very reliable in neutron spectrometry in mixed radiation fields (Thomas and Alevra, 2002; Gomez-Ros et al., 2010).

Currently in Brazil there has been only one calibration laboratory for neutron survey meters which is also responsible for the custody and maintenance of the neutron fluence standard, located at the Brazilian National Metrology Laboratory of Ionizing Radiation (LNMRI), of the Instituto de Radioproteção e Dosimetria (IRD/CNEN), Rio de Janeiro. At the Instituto de Pesquisas Energéticas e Nucleares (IPEN) there are over 20 neutron radiation detectors used by workers at the two nuclear reactors and two cyclotrons, besides various neutron sources, which made it a natural candidate for the establishment of another calibration laboratory for neutron area monitors, in São Paulo (LCN).

In the process of neutron field characterization it is necessary to obtain the neutron spectra, and to determine neutron fluence (the number of neutrons travelling through a small sphere in a time interval) and ambient dose equivalent rates [$\dot{H}^*(10)$] at different source-detector distances (Kim et al., 2001; Bedogni et al., 2014). This type of procedure was performed in several laboratories around the world, where these parameters were obtained through the unfolding process (Vega-Carrillo and Martinez-Ovalle, 2016).

The spectrum unfolding aims to obtain the distribution of neutron fluence as a function of energy. In order to obtain better results, several computational codes have been developed that are still being refined. There are several methods of unfolding (algorithms), which are based on several mathematical principles to obtain the neutron spectrum from the counts measured with the Bonner sphere spectrometer (BSS) (Thomas, 2004). Examples of the various computational codes developed are the Bunki program, which uses a recursive interactive method based on non-linear least squares methods to obtain the spectrum (Lowry and Johnson, 1984); the Maxed program, which applies the principle of the maximum entropy to obtain the spectrum (Reginatto et al., 2002); the Nsduaz program, which employs artificial intelligence techniques, using an algorithm of retro-propagation (Vega-Carrillo et al., 2012), and the NeuraLN program that uses artificial neural networks with a mathematical model inspired by the neural structure of intelligent organisms that acquire knowledge through experience (Lemos, 2009a).

In this work, the characterization of the neutron scattering at the LCN was carried out using the RFM method. The spectra, the radiation energies, the fluence rates, the $\dot{H}^*(10)$ and the conversion factors of fluence in dose $h^*_{\varphi}(10)$ were evaluated at distances of 30 cm–258 cm.

The results obtained led to the limitations and conditions to be observed for calibration work at the laboratory, according to the recommendation of ISO 8529-2 (ISO, 2000).

2. Materials and methods

2.1. Calibration laboratory characteristics

A simplified view of the Neutron Calibration Laboratory (LCN) at IPEN and the set-up used to vary the distance between the detector and the source is shown in Fig. 1.

The LCN is part of the Calibration Laboratory of the Radiation MetrologyCenter/IPEN, with dimensions of 6.88 m × 5.46 m and concrete walls 2.8 m in height with 15 cm of thickness covered by drywall (2 cm thickness). The laboratory's concrete ceiling is 15 cm thick and the granite floor is 5 cm thick.

At the laboratory center is located the 2.60 m long apparatus for the positioning of the detectors with an aluminum base and attachment points which facilitate varying the distance and the height between the source and the detector.

2.2. Isotopic neutron source

An 241AmBe neutron source X3 type manufactured by Amersham International Ltd. was used; it was calibrated at the LNMRI Calibration Laboratory, with an activity of 37 GBq (1 Ci) and a neutron emission rate of $(2.46 \pm 0.06)\ 0.10^6 s^{-1}$. Fig. 2 shows the dimensions of the ^{241}AmBe source used in this work.

Table 1 presents the reference values of ISO 8529-1 [23], which are simulated values in vacuum and in an ideal environment, for energy and $h^*_{\varphi}(10)$ of the 241AmBe source spectra.

For the conversion of neutron fluence into the quantities recommended for radiation protection purposes, the conversion

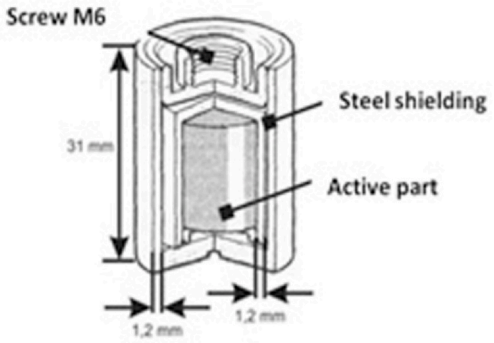

Fig. 2. Neutron source of 241AmBe used at the LCN.

Table 1
Reference values of ISO 8529-1 for energy and $h^*_\varphi(10)$ to the source of ^{241}AmBe (ISO, 2001). These values were obtained through simulation, where the source used was point-typed and in vacuum.

Source	Spectrum average energy (MeV)	h^*_φ (10) (pSv.cm^2)
^{241}AmBe	4.16	391

coefficients $h^*_\varphi(10)$, have been calculated based on the spectra presented in the document ISO 8529-1 (ISO, 2001) and using the fluence to dose equivalent conversion coefficients as a functio n of neutron energy as given in ICRU Report 57 (ICRU, 1998).

2.3. Bonner sphere spectrometer

The Bonner sphere spectrometer (BSS) model 42-5 was manufactured by Ludlum Measurements. This system is composed of spheres of high density polyethylene with diameters of 5.08 cm (2 in), 7.62 cm (3 in), 12.70 cm (5 in), 20.32 cm (8 in), 25.40 cm (10 in) and 30.48 cm (12 in), and by a scintillation detector of ^{6}LiI (Eu) that is comprised of a 4 mm × 4 mm crystal, which is attached to a light guide, which in turn is coupled to a photomultiplier wrapped in an aluminum case (Bramblett et al., 1960).

The electronic system used for this detector consists of an Ortec 142 preamplifier, and a Lynx multi-channel analyzer manufactured by Canberra, which is operated by the Genie 2000 Spectroscopy System program. Through this program the scintillation counting spectra are obtained. The system configuration allows the measurement of neutrons from thermal energies up to 20 MeV; this limitation occurs due to the lack of response function data for energies above this value.

The net counting rate, that is the total counting rate subtracting the background (BG), was measured using the BSS at several source-detector distances ranging from 30 cm to 258 cm. These net counting rates were used as input data to the NeuraLN code, which was used to calculate the spectra, neutron fluence rate and $\dot{H}^*(10)$ at different source-detector distances. The response matrix used was UTA-4, and 81 energy bins were used to determine the spectra (Lemos, 2009b; Vega-Carrillo et al., 2006).

Initially, the correction for attenuation in air was applied, due to the interaction of neutron radiation with oxygen and nitrogen. This attenuation factor F_A (d) is described by Equation (2.1):

$$F_A(d) = \exp(-\overline{\Sigma}.\, d) \tag{2.1}$$

where d is the source-detector distance, expressed in cm, and $\overline{\Sigma}$ is the average linear attenuation coefficient of neutrons by air, obtained by summing the oxygen and nitrogen cross sections weighted by the spectral distribution of the neutrons emitted by the source. The recommended value of $\overline{\Sigma}$ is given by the standard ISO 8529-2 (ISO, 2000).

From the source activity and the neutron emission rate (given in the calibration certificate), it is possible to calculate the direct neutron fluence (without scattering) and $\dot{H}^*(10)$, at different source-detector distances. To determine the direct neutron fluence rate ($\dot{\Phi}$), expressed in n./cm^{-2}.s^{-1}, Equation (2.2) was used:

$$\dot{\Phi} = \frac{S_n}{4.\ \pi.\ d^2} F_1(\Theta)\ F_A(d) \tag{2.2}$$

where S_n is the emission rate of the neutron source (s^{-1}), d is the source-detector distance (cm), F 1(Θ) is the correction factor for source anisotropy, which corrects the neutron fluence as a function of the angle between the direction of the emission considered and the symmetry axis of the source. The anisotropy was measured from a horizontal alignment of the 241AmBe source with the detector at a distance of 2 m, with the source held by a remotely controlled mechanical source rotation system, which was used to rotate the source from 0° to 180°. The anisotropy factor of the source obtained was (1.0288 ± 0.0005). The term $F_A(d)$ is the air attenuation factor mentioned above. The ambient dose equivalent rate $\dot{H}^*(10)$ can be estimated, using Equation (2.3):

$$\dot{H}^*(10) = \Phi \cdot h^*_\Phi \tag{2.3}$$

where $\dot{\Phi}$ is the neutron fluence rate (n/cm^{-2}.s^{-1}), h^*_Φ is the fluence conversion factor for ambient dose equivalent (pSv.cm^2), used for the 241AmBe neutron source and recommended by ISO 8529-2 (ISO, 2000).

2.4. Determination of uncertainties

The uncertainties for the source-detector distances were determined according to the resolution on a metric scale of 1 mm; they were based on the operator experience that the location of one end a given source-detector distance can be set with an uncertainty of approximately 2 mm. Therefore, the uncertainty of the source-detector distance was calculated by means of Equation (2.4):

$$u = \sqrt{u_R{}^2 + u_D{}^2} \tag{2.4}$$

where u_R is the uncertainty related to the resolution of the metallic ruler, $u_R = 1/2\sqrt{6}$; and u_D is the uncertainty associated with the source-detector distance, $u_D = 2/2\sqrt{6}$.

The uncertainties of the fluence rate (theoretical), the ambient dose equivalent rate (theoretical) and the counting rates were determined according to the following expressions:

$$u_c^2 = \sum_{i=1}^{N} \left[\frac{\partial f}{\partial x_i}\right]^2, \text{ where } \frac{\partial f}{\partial x_i} \approx \frac{\Delta f}{\Delta x_i} = c_i \tag{2.5}$$

$$u_c^2 = \sum_{i=1}^{N} [c_i u(x_i)]^2 \tag{2.6}$$

where u_c is the combined uncertainty; c_i is the sensitivity coefficient and $u(x_i)$ is the uncertainty contribution and f is the function of input quantities of the measurement result (GUM, 2012). Table 2 shows an example of the determination of the uncertainties of the fluence rate for the detector-distance of 30 cm.

The model used to express the uncertainties for the ambient dose equivalent rate, averaged energy and fluence values was based on the procedures recommended by the Guide to the Expression of Uncertainty in Measurement (GUM, 2012).

3. Results

Measurements were taken using the BSS system, to obtain the net counting rates (obtained by subtracting the background radiation from the total counting rate data) for each sphere at each of the 13 source-detector distances from 30 cm to 258 cm. Given the count rates observed, 3 h were required to measure a sphere at one location and all

Table 2
Example of the uncertainty for the fluence rate (source-detector distance of 30 cm).

Quantity	Value	Standard uncertainty u(x) k = 1	Sensitivity coefficient |c(x)|	Uncertainty contribution u(x) = u(x)* c(x)
S	2.46 .10 ^{6} s^{-1}	2.8 .10^{4} s^{-1}	9.07.10^{-5} cm^{-2}	2.6
D	30.0 cm	0.5 cm	14.8 $s^{-1}cm^{-3}$	7.4
$F_1(\Theta)$	1.029	0.005	2.17.$10^{}cm^{-2}$ s^{-1}	1.08
F_A (d)	0.99733	0.00004	8.9 .10^{-5} cm^{-2} s^{-1}	3.9.10^{-9}
$\dot{\Phi}$	225.0 n.cm^{-2} s^{-1}			8.0

Table 3
Neutron fluence rates and ambient dose equivalent rates, obtained by calculation using the source emission rates (Theoretical) and by means of the unfolding program NeuraLN applied to the BSS results (total net counting rates) (Experimental).

Source-detector distance (cm)	Theoretical		Experimental	
	Fluence rate $\dot{\Phi}$(n.cm^{-2} s^{-1})	Ambient dose equivalent rate $\dot{H}^*$ (10) (μSv.h^{-1})	Fluence rate $\dot{\Phi}$(n.cm^{-2} s^{-1})	Ambient dose equivalent rate $\dot{H}^*$ (10) (μSv.h^{-1})
30	225.0 ± 8.0	316.3 ± 11.2	261.6 ± 13.1	381.4 ± 19.1
50	81.1 ± 1.9	114.2 ± 2.7	121.3 ± 6.1	176.8 ± 8.8
70	41.5 ± 0.8	58.4 ± 1.1	75.8 ± 3.8	110.5 ± 5.5
90	25.1 ± 0.4	35.4 ± 0.6	54.0 ± 2.7	78.7 ± 3.9
100	20.4 ± 0.32	28.7 ± 0.5	48.6 ± 2.4	70.8 ± 3.5
110	16.9 ± 0.26	23.7 ± 0.36	43.2 ± 2.2	62.9 ± 3.1
130	12.1 ± 0.17	17.0 ± 0.24	37.5 ± 1.9	54.7 ± 2.7
150	9.1 ± 0.13	12.8 ± 0.18	31.8 ± 1.6	46.3 ± 2.3
170	7.1 ± 0.10	10.0 ± 0.13	28.0 ± 1.4	40.0 ± 2.0
190	5.7 ± 0.07	8.0 ± 0.11	24.8 ± 1.2	36.2 ± 1.8
220	4.3 ± 0.05	6.0 ± 0.08	19.4 ± 1.0	28.2 ± 1.4
240	3.6 ± 0.05	5.0 ± 0.06	18.0 ± 0.9	26.2 ± 1.3
258	3.1 ± 0.04	4.4 ± 0.05	15.9 ± 0.8	23.2 ± 1.2

the spheres were measured at all 13 source-detector distances.

Table 3 shows the neutron fluence rates and the $\dot{H}^*(10)$ values, obtained by calculation using the source emission rates and Equations (2.3) and (2.4) (theoretical) and by application of the unfolding program NeuraLN to the BSS measured results to give the total neutron spectrum (direct + scattered) (experimental).

At the source-detector distance of 258 cm the experimental fluence rate values compared to the theoretical ones present a maximum difference of 80.5%. The values of $\dot{H}^*(10)$ present a maximum difference of 81.0% for the source-detector distance of 258 cm, in relation to the theoretical values. This discrepancy between these values occurs due to the scattering of neutron radiation from the floor, ceiling, walls and the irradiation set-up. These additional neutrons make the experimental values greater than the theoretical ones.

During characterization of the neutron field, the spectra, fluence rate and $\dot{H}^*(10)$ were determined at several different positions in the LCN using the total neutron spectrum (direct + scattered) radiation. The values mentioned were obtained by applying the unfolding process performed by the NeuraLN program to the net neutron counting rates registered by each sphere at the several source-detector distances.

Fig. 3 shows log-log and semi-log plots of the total neutron spectrum (direct + scattered) of the 241AmBe neutron source, obtained at different source-detector distances, compared to the reference spectrum from ISO 8529-1 (ISO, 2001). The graphical representation is spectral source strength, BE = dB/dE, vs. energy (ISO, 2001).

Three of the experimental spectra obtained at distances of 30–258 cm of Fig. 3 show that the total spectra changed as compared to the reference spectrum. As the source-detector distance increases, the portion due to scattering also increases because of the interaction between neutrons and the floor, ceiling and walls of the laboratory. Peaks between energies of 10^{-8} MeV and 10^{-4} MeV were observed in the spectra presented at the source-detector distances of 240 cm and 258 cm, due to the scattering caused by the proximity of these locations to the wall.

As just mentioned as the source-detector distance increases, the fraction of the neutron scattering caused by the interaction of the neutrons with floor, ceiling and walls of the laboratory increases too. Thus, it is necessary to characterize the scattered radiation in the LCN, using one of the methods recommended by ISO 8529-2 (ISO, 2000).

Considering the scattering which occurs due to the size of the LCN and the limitations of the several scattering evaluation methods it was decided to use the RFM method, a simplification of the Generalized Fit Method (GFM). The RFM is based on the premise that the minimum distance used has a geometric correction factor close to 1 [$F_1(d) \approx 1$] and that air scattering can be ignored compared to the scattering caused by the experimental set-up; so the RFM can be expressed as (ISO, 2000):

$$M_T(d) = \frac{k}{(d+a)^2} = S \tag{3.1}$$

where $M_T(d)$ is the total device reading, and the parameters k and a (constant values for all distances and spheres) and S (room-scatter contribution) were obtained by adjusting Equation (3.1), of the net counting rates measured with the BSS system at different source-detector distances (d). After proper adjustment, the fractional room-scatter contribution (S) obtained for each sphere was constant that is it did not vary with the source-detector distance. Table 4 shows the S values obtained for each sphere.

To obtain the counting rates for the [$M_D(d)$] term, it was necessary to use Equation (3.1) by setting S = 0 and using only the parameters k and a.

The contribution of the scattered neutrons measured by each BSS system sphere at the source-detector distances from 30 cm to 258 cm was adjusted using Equation (3.1) and the RFM method. Fig. 4 shows experimental data with background subtracted (net curves) compared to those obtained using the RFM method (direct curves), for neutrons detected directly by the bare detector and by the detector within spheres with diameters from 2 in to 12 in, varying the source-detector distance from 30 cm to 258 cm. The curves were fitted using an exponential equation of the type $y = y_0 + A*\exp(R_0*x)$. The R^2 values for these fits are also shown.

The results presented in Fig. 4 show that the counting rates due to the direct neutrons (without scattering) determined with the RFM method give better fits than the experimental net counting rates. Further note that the improvement due to the RFM method increases as the size of the thermal sphere increases, due to the growing sensitivity of the detector to thermal neutrons.

Table 5 presents the values obtained for energy, fluence rate, $\dot{H}^*(10)$ and $h^*_{\varphi}(10)$ in different positions of the LCN, due to the direct and scattered neutrons. These results were calculated with the NeuraLN program from the counting rates determined via the RFM method at different source-detector distances as shown in Fig. 4. The parameters, fluence rates and $\dot{H}^*(10)$, presented in Table 5, were obtained by means of the experimental method (previously described); they may be compared with the data obtained by the calculation (theoretical) method, which can be observed in Table 3.

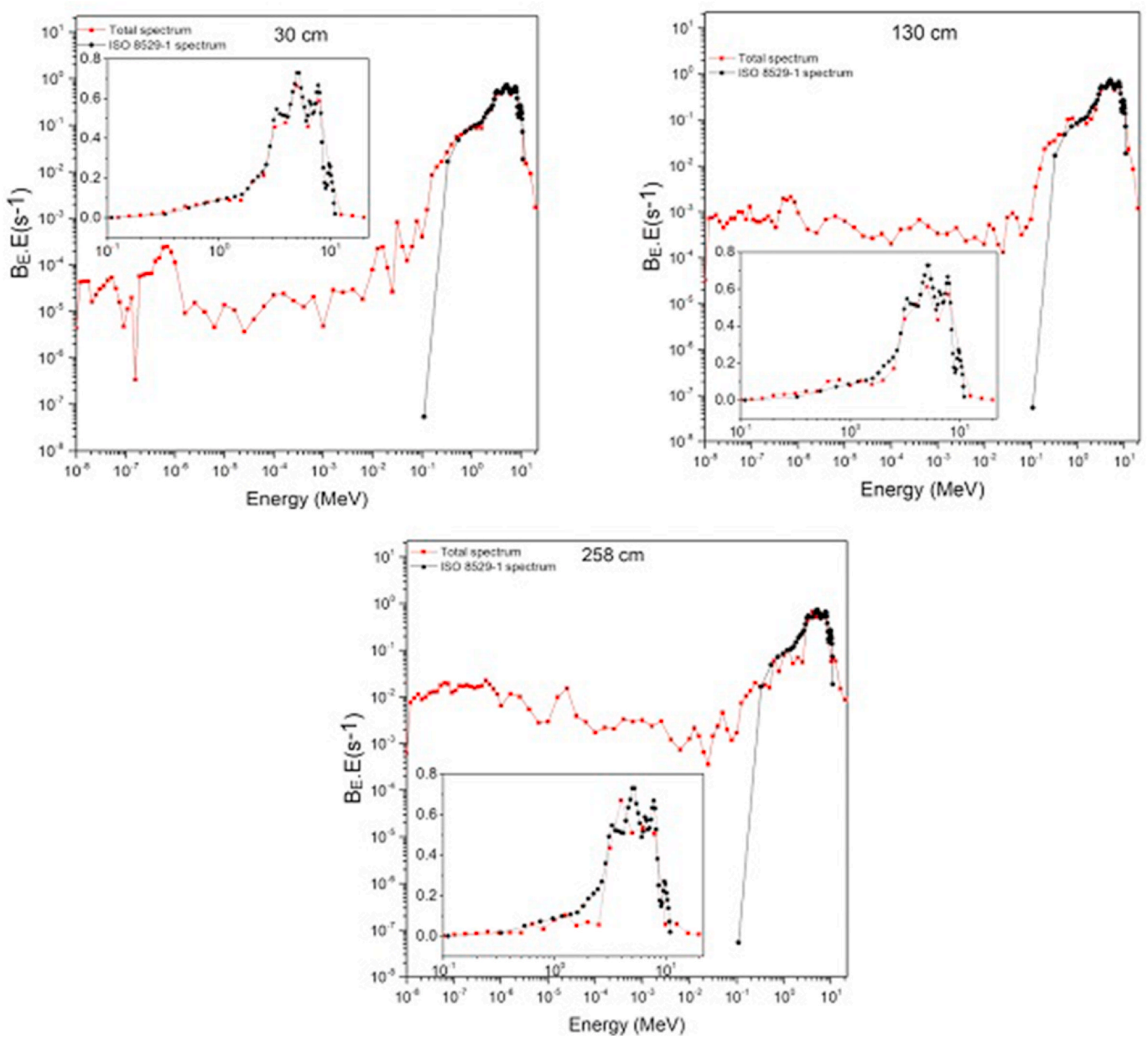

Fig. 3. Total neutron spectra (direct + scattered) radiation of the 241AmBe neutron source [red dots], obtained at three different source-detector distances, compared to the reference spectrum ISO 8529-1 (ISO, 2001) [black dots]. (For interpretation of the references to colour in this figure legend, the reader is referred to the Web version of this article.)

Table 4
Constant values of S obtained by application of Equation (3.1), using the bare detector and the spheres with different diameters.

Sphere Diameter (inch)	S
0	0.23 ± 0.01
2	0.45 ± 0.01
3	0.15 ± 0.04
5	0.95 ± 0.07
8	0.73 ± 0.07
10	0.80 ± 0.11
12	0.62 ± 0.09

The results from the RFM derived direct neutrons presented in Table 5 show that the fluence rates present a maximum percentage difference, when compared to the calculated values presented in Table 3, of 2.4% for the source-detector distance of 220 cm, and the values $\dot{H}^*(10)$ presented a difference of 2.3% for the source-detector distance of 258 cm. The energy values obtained experimentally present a percentage difference of 1.0%. The source-detector distance of 258 cm and the values of $h^*_{\varphi}(10)$ showed a percentage difference of 0.3% relative to the reference values presented in Table 1.

Fig. 5 shows the direct and scattered neutron spectra of the 241AmBe source, produced by the NeuraLN program operating on data from each sphere at different source-detector distance. The reference spectra of ISO 8529-1 (ISO, 2001) are shown for comparison. The graphical representation is spectral source strength, BE = dB/dE vs. energy (ISO, 2001).

The reference spectrum (from ISO 8529-1) and the spectra by application of the RFM method from 30 cm to 258 cm, present similarities that demonstrate that the RFM method is effective in determining scattering in the LCN. The spectra acquired using the scattered counting

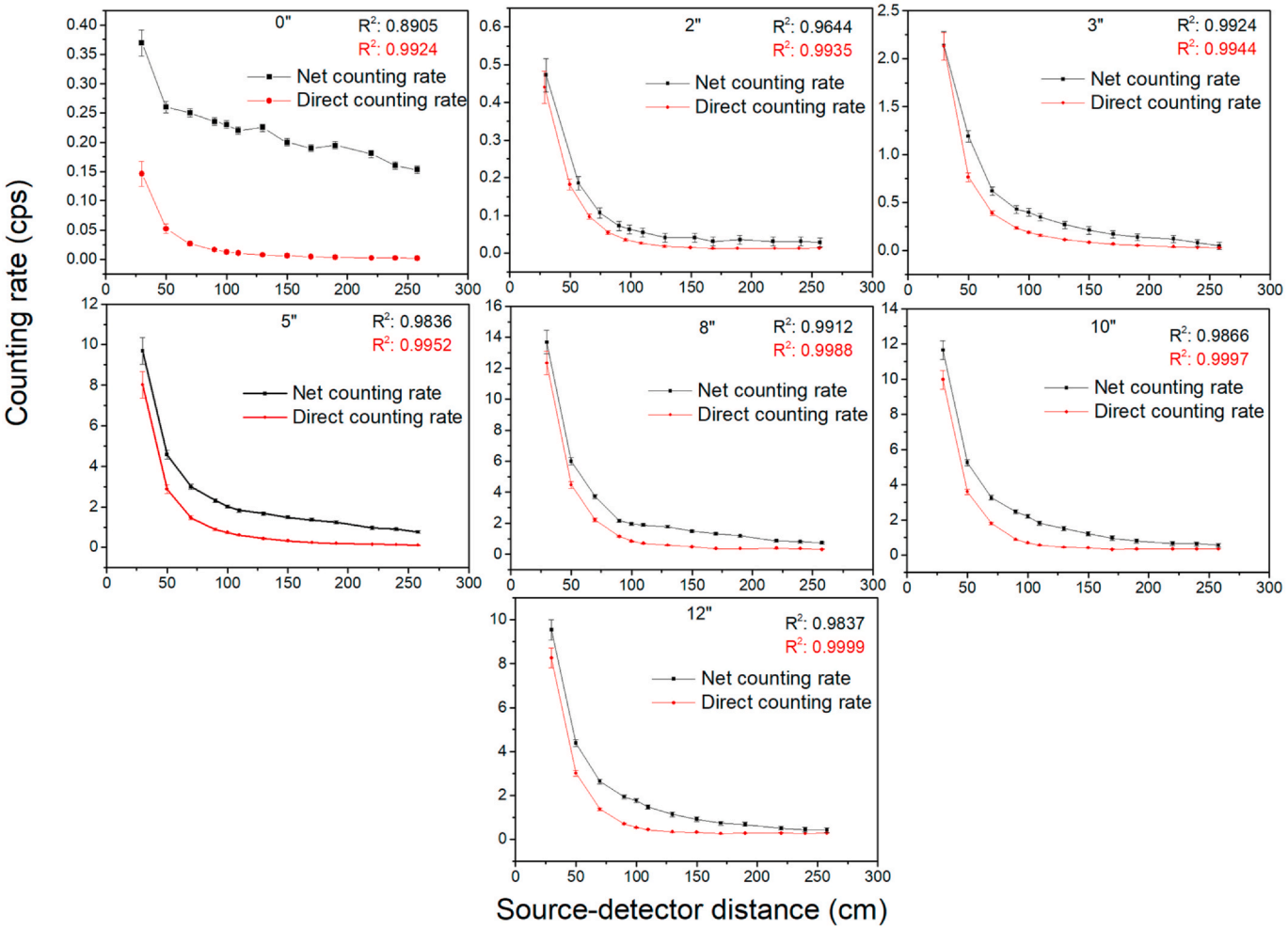

Fig. 4. Counting rates due to the net neutrons (i.e. background subtracted) from the source measured by the BSS spheres and direct neutron curves resulting from application of the RFM method. The maximum uncertainty was 2.5%, not visible in the curves.

rates showed significant changes for the measurement positions located near the walls at the source-detector distances of 130 cm–258 cm when compared with the direct and reference spectra ISO 8529-1 (ISO, 2001).

In these positions interaction of the neutrons with the walls, floor and ceiling of the LCN cause the appearance of peaks between the energies of 10^{-8} MeV and 10^{-2} MeV in the spectra due to the neutron scattering.

The scattering fraction for fluence rate and $\dot{H}^*(10)$ at the different source-detector distances were determined by adjusting Equation (3.1), using the experimental values presented in Table 3, when determining the value of fractional room-scatter contribution (S) in each distance source-detector, which was S = 14.11 ± 1.22 at all positions used. In order to determine the scattering fraction at different distances, it is necessary to use Equation (3.2)

Table 5
Results obtained by the NeuraLN program for energy, fluence rate, $\dot{H}^*$ (10) and $h^*_{\varphi}(10)$ at different positions of the LCN, using the direct neutron counting rates (Alvarenga, 2018).

Source-detector distance (cm)	Energy (MeV)	Fluence rate (n.cm^2.s^{-1})	$\dot{H}^*$ (10) (μSv/h)	h^*_{φ} (10) (pSv.cm^2)
30	4.20 ± 0.21	227.5 ± 11.4	320.3 ± 16.0	392 ± 20
50	4.20 ± 0.21	81.7 ± 4.1	114.9 ± 5.7	392 ± 20
70	4.20 ± 0.21	41.6 ± 2.1	58.6 ± 2.9	392 ± 20
90	4.20 ± 0.21	25.2 ± 1.3	35.4 ± 1.8	392 ± 20
100	4.20 ± 0.21	20.4 ± 1.0	28.7 ± 1.4	392 ± 20
110	4.20 ± 0.21	16.8 ± 0.8	23.7 ± 1.2	392 ± 20
130	4.20 ± 0.21	12.0 ± 0.6	17.0 ± 0.8	392 ± 20
150	4.20 ± 0.21	9.0 ± 0.5	12.7 ± 0.6	392 ± 20
170	4.20 ± 0.21	7.0 ± 0.4	9.9 ± 0.5	392 ± 20
190	4.20 ± 0.21	5.6 ± 0.3	7.9 ± 0.4	392 ± 20
220	4.20 ± 0.21	4.2 ± 0.2	5.9 ± 0.3	392 ± 20
240	4.20 ± 0.21	3.5 ± 0.2	5.0 ± 0.2	392 ± 20
258	4.21 ± 0.21	3.1 ± 0.2	4.3 ± 0.2	392 ± 20

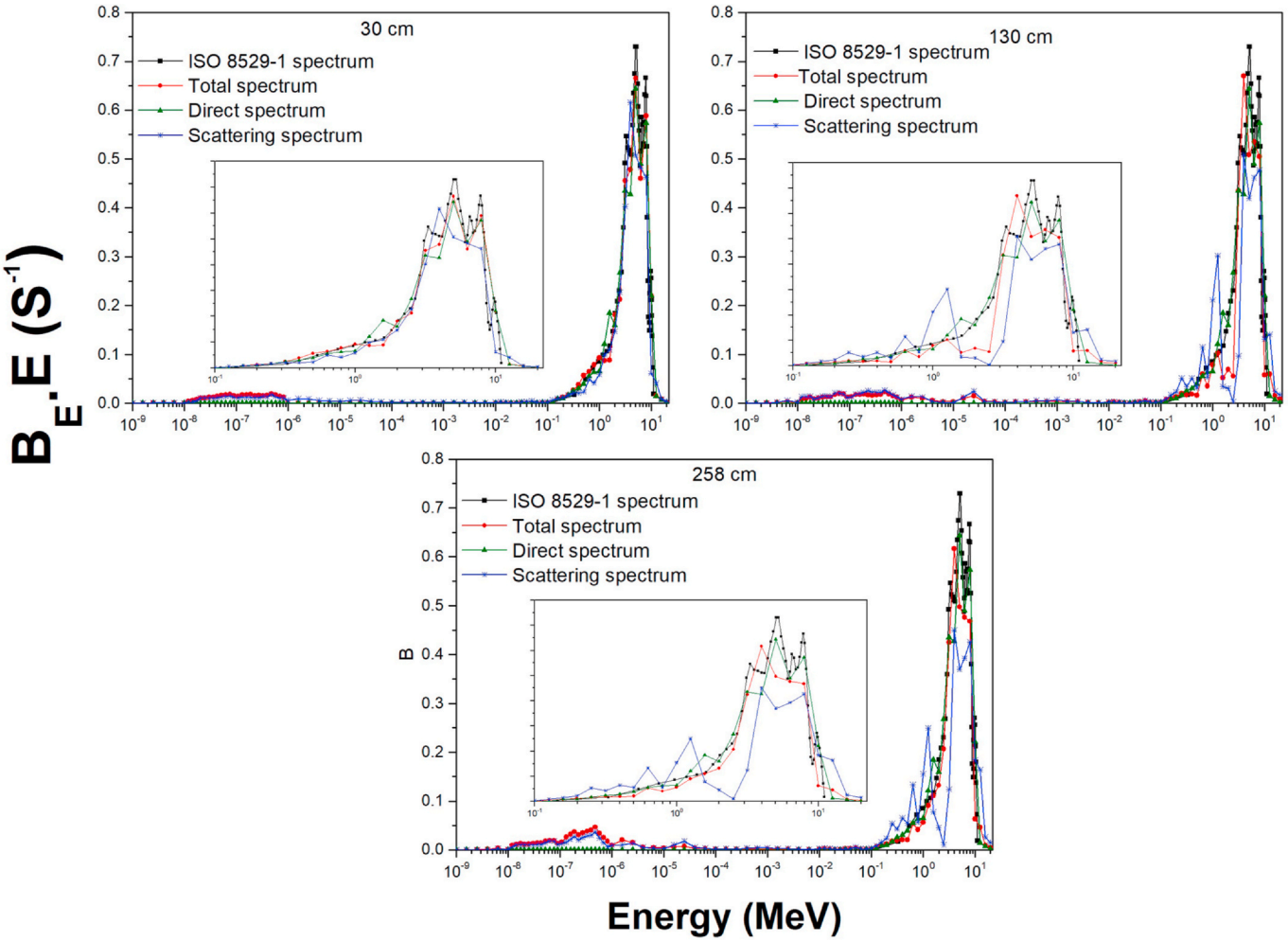

Fig. 5. Direct, scattered and total (direct + scattered) neutron spectra of the 241AmBe neutron source, obtained at different source-detector distances from 30 cm to 258 cm, compared to the reference spectrum of ISO 8529-1 (ISO, 2001).

$$S_F = \frac{S}{\Phi} \tag{3.2}$$

where S_F is the scattering fraction at a given distance, S is the fractional room-scatter contribution and Φ is the experimental fluence rate or $\dot{H}^*(10)$. The results obtained are shown in Table 6. The scattering fraction values were determined at distances from 30 cm to 258 cm from the fluence rate and the ambient dose equivalent rate.

Table 6
Scattering fraction for fluence rate and $\dot{H}^*(10)$, obtained for source-detector distances of 30 cm–258 cm.

Source-detector distance (cm)	Scattering fraction	
	Fluence rate (%)	$\dot{H}^*$ (10) (%)
30	6	4
50	15	10
70	25	18
90	36	26
100	41	29
110	46	32
130	54	38
150	61	43
170	67	47
190	71	51
220	77	55
240	80	57
258	82	58

As observed in Table 6, the highest scattering fraction for fluence rate was 82% at the source-detector distance of 258 cm, and for $\dot{H}^*(10)$ the highest scatter fraction was 58%, also at the source–detector distance of 258 cm.

Thus, the scattering radiation increases as the source-detector distance increases and in the geometry of the LCN the source is located at the center. From ISO 8529-2 (ISO, 2000), the scattering contribution must not exceed 40% at the calibration point; thus, at the source-detector distances of 30 cm, 50 cm, 70 cm and 90 cm, the scattering contribution is within the recommended limit.

4. Conclusions

In this study the LCN neutron fields were characterized. The spectra, fluence rate and $\dot{H}^*(10)$ were determined for a central source and several source-detector distances with the objective of showing and correcting for scattered radiation. As the source-detector distance increases, the scattered radiation caused by the interaction of the neutrons with floor, ceiling and walls of the laboratory increases too. Thus, it was necessary to characterize the radiation scattering in the LCN, using one of the methods recommended by ISO 8529-2 (ISO, 2000).

For the neutron radiation field characterization of the LCN the scattering of neutrons was evaluated by means of the Reduced-Fitting Method recommended by ISO 8529-2 (ISO, 2000). The direct neutron spectra were determined at various source-detector distances.

The direct neutron spectra were similar in form to the reference spectrum (ISO 8529-1) (ISO, 2001), and the scattered spectra showed significant changes in relation to the reference spectrum, especially in the measurement positions near the laboratory wall. The scattering fraction values were determined at distances from 30 cm to 258 cm from the fluence rate and from the ambient dose equivalent rate. The results show that at distances of 90 cm and less, the contribution of neutron scattering is within the recommended values of ISO 8529-2 (ISO, 2000).

Declaration of competing interest

The authors declare that they have no known competing financial interests or personal relationships that could have appeared to influence the work reported in this paper.

Acknowledgments

The authors acknowledge the Brazilian agencies CNPq (Grant No. 301335/2016-8) and CNEN (Grant No. 01342.002316/2019-46) for partial financial support, and Dr. Evaldo S. da Fonseca, of the Instituto de Radioproteção e Dosimetria, IRD/CNEN, Rio de Janeiro, Brazil, for important suggestions.

References

Alvarenga, T.S., Federico, C.A., Caldas, L.V.E., 2017. Determination of radiation spread in the IPEN neutron calibration laboratory. Braz. J. Radiat. Sci 5, 1–10.

Alvarenga, T.S., 2018. Establishment and characterization of a calibration laboratory with reference neutron beams and traceability to the international metrology system. PhD Thesis – Programa de Pós-Graduação em Tecnologia Nuclear. Instituto de Pesquisas Energéticas e Nucleares – IPEN-CNEN/SP, University of São Paulo, Brazil (In Portuguese).

Antanackovic, T., Yonkeu, A., Dubeau, J., Witharana, H.S., Priest, N., 2015. Characterization of neutron fields from bare and heavy water moderated 252Cf spontaneous fission source using Bonner sphere spectrometer. Appl. Radiat. Isot. 99, 122–132.

Bedogni, R., Domingo, C., Roberts, N., Thomas, D.J., Chiti, M., Esposito, A., Garcia, M.J., Gentile, A., Liu, Z.Z., de San-Pedro, M., 2014. Investigation of the neutron spectrum of americium-beryllium sources by Bonner sphere spectrometry. Nucl. Instrum. Methods Phys. Res., Sect. A 763, 547–552.

Bramblett, R.L., Ewing, R.I., Bonner, T.W., 1960. A new type of neutron spectrometer. Nucl. Instrum. Methods Phys. Res. 9, 1–12.

Dawn, S., Bakshi, A.K., Sathian, D., Selvam, T.P., 2016. Estimation of neutron scatter correction for calibration of personnel dosimeter and dose ratemeter against 241Am-Be source - Monte Carlo simulation and measurements. Radiat. Protect. Dosim. 175 (2), 149–162.

Gomez-Ros, J.M., Bedogni, R., Moraleda, M., 2010. Design and validation of a single sphere multi-detector neutron spectrometer based on LiF:Mg,Cu,P thermoluminescent dosemeters. Radiat. Meas. 45, 1220–1223.

Gressier, V., 2014. Review of neutron calibration facilities and monitoring techniques: new needs for emerging fields. Radiat. Protect. Dosim. 161 (1–4), 27–36.

GUM, 2012. Guide to the expression of uncertainty in measurement. The role of measurement uncertainty in conformity assessment. Joint committee for guides in metrology. JCGM 106.

Hwan, B.K., Lyul, J.K., Young, S.C., Cho, G., 2014. Scattered neutron calibration fields of KAERI. J. Nucl. Sci. Technol. 37, 781–784.

ICRU, 1998. International Standard. Conversion Coefficients for Use in Radiological Protection against External Radiation, vol. 57 Report, Bethesda.

ISO, 2000. International Standard. Reference Neutron Radiations – Part 2: Calibration Fundamentals of Radiation Protection Devices Related to the Basic Quantities Characterizing the Radiation Field (Geneva). first ed. Report 8529-2.

ISO, 2001. International Standard. Reference Neutron Radiations – Part 1: Characteristics and Methods of Production (Geneva). first ed. Report 8529-1.

Kim, B.-H., Kim, J.-L., Chang, S.-Y., Cho, G., 2001. Characteristics of the KAERI neutron reference fields for the calibration of neutron monitoring instruments. J. Korean Assoc. Radiat. Prot. 26 (3), 243–248.

Kluge, H., Alevra, A.V., Jetzke, S., Knauf, K., Matzke, M., Weise, K., Wittstock, J., 1997. Scattered neutron reference fields produced by radionuclide sources. Radiat. Protect. Dosim. 70 (1–4), 327–330.

Le, T.N., Tran, H.N., Nguyen, K.T., Trinh, G.V., 2017. Neutron calibration field of a bare 252Cf source in Vietnam. Nucl. Eng. Technol. 49, 277–284.

Lee, S.K., Kim, S.I., Lee, J., Chang, I., Kim, J.L., Kim, H., Kim, M.C., Kim, B.H., 2018. Evaluation of neutron scattering correction using the semi-empirical method and the shadow-cone method for the neutron field of the korea atomic energy research institute. Radiat. Protect. Dosim. 180 (1–4), 46–50.

Lemos, M.R., 2009a. Neutron spectra unfolding using Monte Carlo Method and artificial neural networks. PhD Thesis – Programa de Pós-Graduação em Energia Nuclear (COPPE). Federal University of Rio de Janeiro, COPPE, Brazil (In Portuguese).

Lemos, M.R., 2009b. Development of an answer matrix for the bonner multisphone spectrometer. Braz. J. Radiat. Sci. 7, 1–5.

Lowry, K.A., Johnson, T.L., 1984. Modifications to Iterative Recursion Unfolding Algorithms and Computer Codes to Find More Appropriate Neutron Spectra (Washington, D. C., USA). NRL Memorandum Report, vol. 5340.

Reginatto, M., Goldhagen, P., Neumann, S., 2002. Spectrum unfolding, sensitivity analysis and propagation of uncertainties with the maximum entropy deconvolution code MAXED. Nucl. Instrum. Methods Phys. Res., Sect. A 476, 242–246.

Schuhmacher, H., 2004. Neutron calibration facility. Radiat. Protect. Dosim. 110, 33–42.

Thomas, D.J., 2004. Neutron spectrometry for radiation protection. Radiat. Protect. Dosim. 110, 141–149.

Thomas, D.J., Alevra, A.V., 2002. Bonner sphere spectrometers - a critical review. Nucl. Instrum. Methods Phys. Res. 476, 12–20.

Thiem, N.L., Hoai-Nam, T., Khai, T.N., Giap, V.T., 2017. Neutron calibration field of a bare 252Cf source in Vietnam. Nucl. Eng.Technol. 49, 227–284.

Vega-Carrillo, H.R., Manzanares-Acuña, E., Iñiguez, M.P., Gallego, E., Lorente, A., 2007a. Spectrum of isotopic neutron sources inside concrete wall spherical cavities. Radiat. Meas. 42 (8), 1373–1379.

Vega-Carrillo, H.R., Manzanares-Acuña, E., Iñiguez, M.P., Gallego, E., Lorente, A., 2007b. Study of room-return neutrons. Radiat. Meas. 42 (3), 413–418.

Vega-Carrillo, H.R., Ortiz-Rodrigues, M.J., Martínez-Blanco, M.R., 2012. NSDUAZ unfolding package for neutron spectrometry and dosimetry with Bonner spheres. Appl. Radiat. Isot. 71, 87–91.

Vega-Carrillo, H.R., Hernández-Dávila, M.V., Manzanares-Acuña, E., Mercado, G.A., Iñiguez, M.P., Barquero, R., Palacios, P., Villafañe, R.M., Arteaga, T.A., Rodriguez, J.M.O., 2006. Neutron spectrometry using artificial neural networks. Radiat. Meas. 41, 425–431.

Vega-Carrillo, H.R., Martinez-Ovalle, S.A., 2016. Few groups neutron spectra, and dosimetric features, of isotopic neutron sources. Appl. Radiat. Isot. 117, 42–50.